Banding of suspended particles in a rotating fluid-filled horizontal cylinder

G. Seiden,[1,*] M. Ungarish,[2] and S. G. Lipson[1]
[1]*Department of Physics, Technion-Israel Institute of Technology, 32000 Haifa, Israel*
[2]*Department of Computer Science, Technion-Israel Institute of Technology, 32000 Haifa, Israel*
(Received 30 December 2004; revised manuscript received 1 June 2005; published 29 August 2005)

Non-Brownian particles suspended at low volume concentration in a rotating horizontal cylinder filled with a low-viscosity fluid are observed to segregate into well-defined periodic axial bands. We present an experimental investigation of the dependence of the phenomenon on particle characteristics, tube diameter and length, and fluid viscosity. A theoretical explanation of the phenomenon is suggested, in which the segregation occurs as a result of mutual interaction between the particles and inertial waves excited in the bounded fluid. This leads to the result that macroscopic suspended particles accumulate in alternate nodes of the wave excitation, which is in agreement with the experiments, and leads to two degenerate band patterns for each mode. Under some conditions the observed pattern oscillates between the two possible band configurations. The mechanism underlying the oscillations is unclear. A confirmation of the theoretical approach was obtained by means of a photographic capture of the flow field resulting from the inertial waves.

DOI: 10.1103/PhysRevE.72.021407 PACS number(s): 82.70.−y, 47.55.Kf, 47.35.+i, 47.54.+r

I. INTRODUCTION

The rotating horizontal tube partially or completely filled with a mixture of fluid and solid particles presents a fertile ground for a variety of pattern-formation phenomena. Recent years have seen extensive experimental and theoretical investigations into the different self-organizing systems, the most intensively studied being the banding phenomenon occurring in a mixture of two or more granular materials either in air [1] or within a fluid [2]. Yet another example is the segregation into axial bands of neutrally buoyant particles contained in a viscous suspension which partially fills either the available volume between two concentric horizontal cylinders (the outer cylinder being at rest while the inner rotates at constant frequency) [3], or a rotating horizontal tube [4].

The banding of a dilute suspension containing non-Brownian particles in a fluid that fills a rotating horizontal cylinder was first observed several years ago during research into the influence of anisotropy on the growth of dendritic crystals [5]. In order to prevent the crystals from interacting with a substrate, a supersaturated solution of NH_4Cl was placed in a horizontal cylinder which was then rotated about its axis with a constant angular frequency, thus attaining levitation during which the growth could be examined. As the crystals nucleated, a surprising tendency to accumulate at specific, periodically spaced bands was observed (Fig. 1).

Preliminary experimental investigations of the phenomenon were carried out indicating a widespread phenomenon, occurring for a large range of particle size and of solution viscosity. Lipson and Seiden [6] observed the phenomenon for millimeter-sized plastic particles and air bubbles, as well as for aluminum flakes of the order of 100 μm, suspended in water. Breu *et al.* [7] reported the banding phenomenon for a dilute aqueous suspension containing 100 μm glass beads. In both cases the dominant periodic spacing between consecutive bands was approximately $3.5R-4R$ (R is the tube radius), though for the smaller particles instances with periods equal to approximately half the above spacing were also observed. Matson *et al.* [8] carried out experiments with 100 μm glass beads suspended in various water-glycerol solutions and reported a periodic spacing of approximately $2.4R$. With regard to the latter work, an attempt to explain the banding mechanism was reported by Lee and Ladd [9], based on particle-particle interaction in the low Reynolds number regime. The Reynolds number referred to is $\mathrm{Re}=dU_{rel}\rho/\eta$, where d is a typical particle dimension, U_{rel} its relative velocity with respect to the fluid, and ρ and η are the fluid density and dynamic viscosity, respectively. The periodic spacing anticipated by their theory, taking into account the important screening effect of the bounding cylinder, was $1.4R$. Experiments on growing NH_4Cl crystals [5,6] were more ambivalent and have shown two tendencies, $2.5R$ and $3.8R$. The fact that crystals of a large range of sizes grew simultaneously makes the interpretation of these experiments difficult.

The present paper, in part an expanded account of a previously published communication [10], concerns an extensive experimental investigation, complemented by a theoretical analysis, into the main characteristics of the banding phenomenon, focusing mainly on the low viscosity limit. The

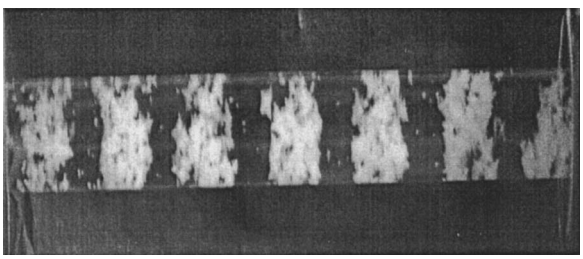

FIG. 1. Banding phenomenon of NH_4Cl crystals in their supersaturated solution (from Lipson [5]).

*Corresponding author. Email address: seideng@techunix.technion.ac.il

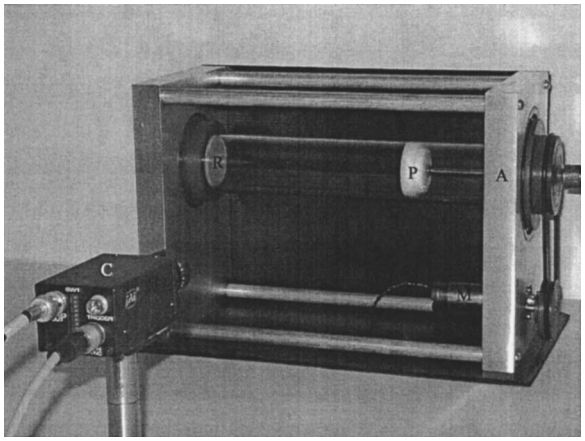

FIG. 2. The experimental system used to rotate glass tubes about their axis for the investigation of the banding phenomenon. A is the aluminum stand, P the teflon piston, R the rubber plug, and M the motor. C is the charged-coupled-device (CCD) camera used to record the phenomenon.

results of the experimental investigation, presented in Sec. II, indicate a robust phenomenon independent to a large extent on particle characteristics and scaling with the tube diameter. The dependence on the finite length of the tube, which was not considered in previous experiments, turned out to be crucially important. The theoretical approach, based on the assumptions of linearity (i.e., small perturbation to the otherwise rigidly rotating fluid) and low viscosity, whereby the segregation into bands results from a mutual interaction between the gravity-induced motion of the suspended particles and excited inertial waves in the bounded rotating fluid, is presented in Sec. III. Experimental confirmation of the theoretical result, in the form of a photographic capture of the flow field pertaining to the banding phenomenon, is presented in Sec. IV. Finally, in Sec. V, we discuss the limits of the theoretical framework with regard to nonlinear and viscous effects which were neglected in the theory.

II. EXPERIMENTAL INVESTIGATION

A. Experimental setup

The experimental apparatus used is a basic mechanical system designed to rotate glass tubes about their horizontal axis (Fig. 2). The system consists of two aluminum supports upon which a pair of 70 mm (inner diameter) bearings are mounted. The supports are fastened together with four aluminum rods. A glass tube is tightly fixed to the bearings on both ends by PVC sleeves and is driven by a rubber O-ring from a dc motor. The glass tube contains a piston that allows the tube length to be varied. The opposite end, used to fill the tubes with the fluid and particles, is either closed with a rubber plug (Secs. II B and II D) or made of transparent material to allow investigation of the phenomenon in the vertical plane perpendicular to the axis of rotation (Secs. II C and II E). The particles used in the different sets of experiments were either purchased (primarily from Polysciences, Inc.) or were made in our mechanical workshop. Specific details of the particles, tubes, rotation rates, and fluid viscosity employed in the different experiments are given in the sections below.

The phenomenon was recorded on tape using a charge-coupled-device (CCD) camera which was placed either at right angles to the axis of rotation (Secs. II B and II D) or on the axis, facing one of the tube ends (Secs. II C and II E). The recorded tape was then digitally analyzed (Secs. II B, II D, and II E) or used for illustration as a video clip [11].

B. Dependence of banding period on tube length

Four sets of experiments were carried out in water ($\eta \cong 1$ cP). In each set the tube length was varied at intervals of a few millimeters over a total range of several tube diameters. For every tube length the phenomenon was recorded via a CCD camera facing the vertical plane through the axis of rotation (Fig. 2). Different particles and/or tube diameter were used in each set in order to further study the effect of particle characteristics and tube diameter on the phenomenon. The volume fraction (disperse phase volume/total volume) was kept constant in each set, and was in general of the order of 1%. Table I shows details of particle characteristics, tube diameter and length-range, and frequency of rotation, which were used in the different sets.

The recorded tape of each experiment, lasting a few minutes, was analyzed as follows: Ten individual frames (gray-

TABLE I. Details of the parameters used in each of the four sets of experiments.

Set	Particle	Dimensions (mm)	Specific gravity	Volume fraction (%)	Tube diameter (mm)	Tube length range (mm)	Rotation frequency (Hz)
1	Polystyrene ball	$d=3$	1.05	1.27	44.5	70–200	1.00
2	Perspex cube	$a=2$	1.18	0.51	44.5	70–200	1.54
3	Perspex cylinder	$d=1$, $l=2$	1.18	0.61	25.7	40–165	1.42
4	Nylon ball	$d=1.5$	1.11	1.02	25.7	40–177	1.20

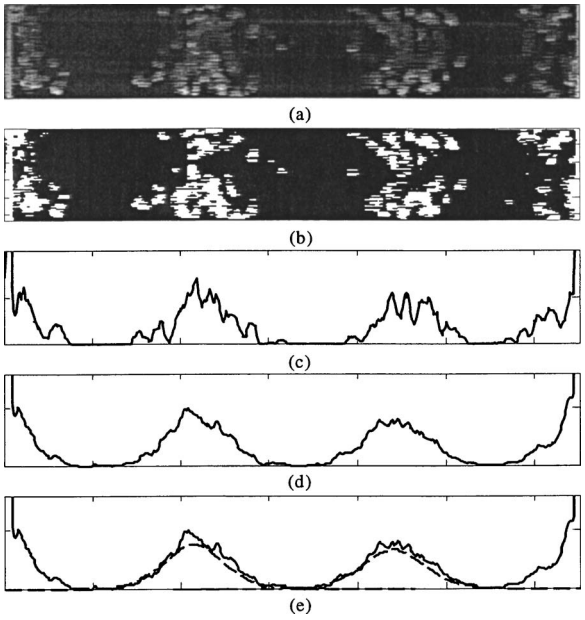

FIG. 3. Successive stages in the analysis of the ten frames taken for each tube-length illustrated for Perspex cylinders at $L = 130$ mm (third set): (a) One of the ten frames entered into the computer program. (b) Converted into black and white array. (c) Column-intensity graph for the particular frame. (d) Mean column-intensity graph for the ten frames. (e) Fitting the bands using a Gaussian curve (broken line).

scale images) were extracted at intervals of about 10 s^1 [Fig. 3(a)] and entered into a computer program. The program converted each frame into a black and white array[2] [Fig. 3(b)]. It then provided a column-intensity graph (summing vertically) for each frame [Fig. 3(c)] and finally provided a mean column-intensity graph of the ten frames [Fig. 3(d)]. Another computer program calculated the mean position of the peak of each band in the tube using a Gaussian fit [Fig. 3(e)]. This provided a measurement of the periodic length.

In all the experiments it appeared that the exact value of the rotation frequency was not important, provided that it lay between two extremes. At the lower end, the frequency must be high enough to levitate the particles so that they remain in suspension. At the upper end, the frequency must not be so high as to pin the particles to the tube wall by centrifugal effects. The results of the four sets are presented in the generic graph of Fig. 4, where both the tube length and periodic length are scaled by tube radius. Apart from minor deviations we see the same sawtoothlike dependence of the periodic length on tube length, with the data generally falling on the straight lines (dashed lines in Fig. 4):

$$L = n\frac{\Lambda}{2}, \quad n = 2,3,4, \ldots,$$

here L is the tube length and Λ the periodic length.

[1]The time interval between successive frames was in some instances affected by the stability of the band patterns (e.g., oscillations between two possible patterns).

[2]The grayscale threshold level used in the conversion corresponded to the maximal background illumination.

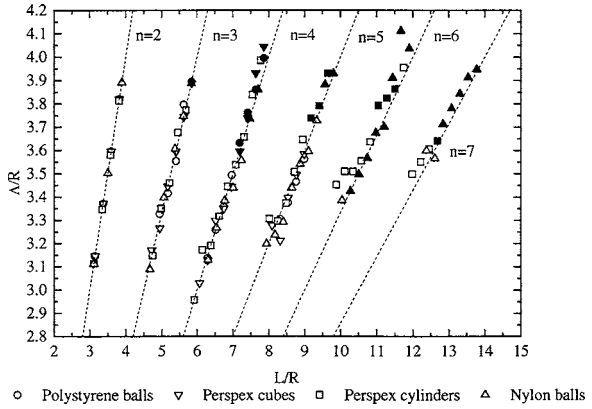

FIG. 4. Summary of all data gathered in the investigation of the dependence of periodic length on tube length (both scaled by tube radius) for particles suspended in water, manifesting general features of the banding phenomenon. The solid symbols indicate oscillating patterns (discussed in Sec. II C).

In all sets it can be seen that for relatively short tube lengths there is a gap between two successive slopes in which the bands did not form at all. It is also worth noting that for long tubes there seems to be a convergence of the periodic length to a value of four times the tube radius. The dominant periodic lengths in the experiments done by Lipson and Seiden [6] and by Breu *et al.* [7] are in agreement with the above graph.

C. Oscillations

Another important observation concerns the position of bands relative to the bounding perpendicular walls of the cylinder: at the walls there can either be a band or the midplane between two bands (see Fig. 5), thus allowing for two possible states of the system. This last fact is manifested in an unexpected phenomenon of oscillation between two possible configurations. Situations where this occurred are represented by the solid symbols in Fig. 4. These oscillations resemble the well-known oscillations between two coupled pendulums from classical mechanics and the Rabi oscillations between two coupled states in quantum mechanics. They were observed at analogous points in all the sets of data and can be seen to be mainly above the average periodic length ($\cong 3.6R$). In Fig. 6 we present two periods of oscillations for the case of polystyrene balls oscillating between the two possible states at $L = 16.5$ cm [a video clip of the oscillating bands is also available (Ref. [11])]. The time period in

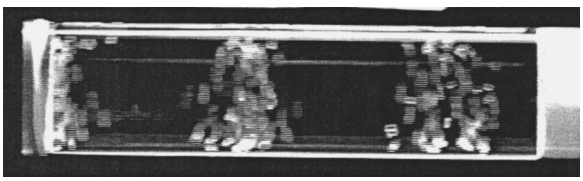

FIG. 5. Two boundary conditions manifested for Perspex cylinders suspended in water at $L = 11.2$ cm. For these boundary conditions a degenerate state with bands shifted half a period to the right also exists.

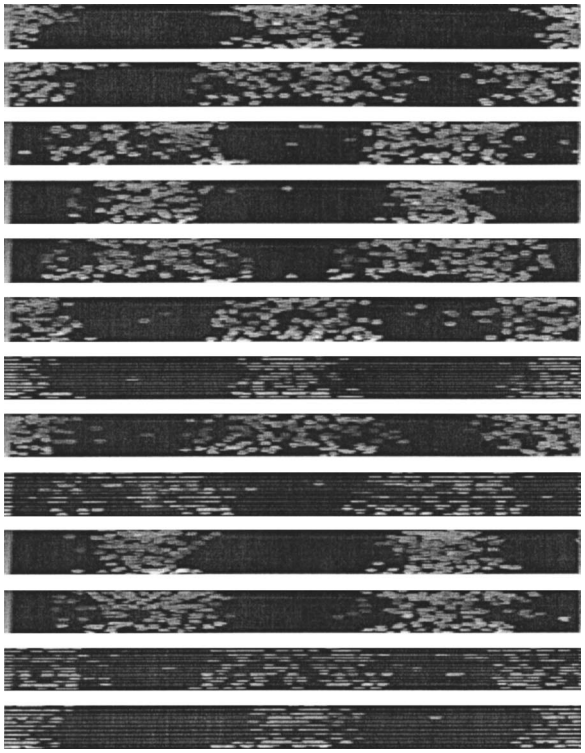

FIG. 6. Polystyrene balls suspended in a water-filled 44.5 mm (inner diameter) tube oscillating between two allowed states at $L = 16.5$ cm. Note that the middle band splits in two in order to form the new bands (and vice versa). The interval between successive frames is 3.5 s.

this specific case is approximately 21 s. Note that the tube length in this instance is equal to twice the periodic length.

We further examined the development of the oscillating bands by placing the CCD camera toward one of the bounding walls of another tube (having an inner diameter equal to 58 mm), which was in this case sealed with a transparent window. Figure 7 shows two stages in the dynamical development of the phenomenon. When well-defined the bands are characterized by off-centered rings [Fig. 7(a)]. They then contract [Fig. 7(b)] before splitting and merging with adjacent bands.

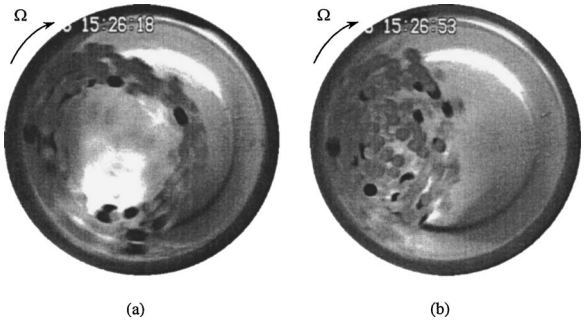

FIG. 7. End view showing two main stages in the development of the oscillating bands (a) off-centered rings when the bands are well-defined, and (b) bands contract just before splitting.

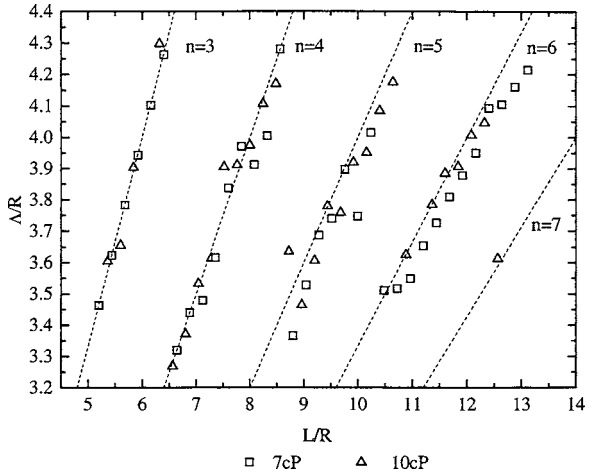

FIG. 8. Dependence of the periodic length on tube length (both scaled by tube radius) for 1 mm glass beads suspended in water-glycerol solutions.

D. Higher viscosities

In order to investigate the influence of viscosity we have carried out two experiments similar to the ones described in Sec. II B, with higher values of fluid viscosity. The particles used were 1 mm glass beads, suspended in a water-glycerol solution. The reason for using glass beads lies in the relatively high specific gravity ($\cong 2.5$) of glass—a fact that enabled us to work with high glycerol concentrations without the particles becoming neutrally buoyant. We present in Fig. 8 the results of the two sets of experiments done with solution viscosities of 7 and 10 cP (56% and 62% glycerol by weight, respectively, at 25 °C). The volume fraction in both cases was 0.74% and the tube's inner diameter was 25 mm.

The data show no significant difference between these results and the results obtained with water ($\eta \cong 1$ cP), other than that the average periodic length corresponding to Fig. 8 is slightly greater, and that there were no oscillations observed in these experiments. Nevertheless, for values of viscosity higher than 10 cP we noticed an increasing tendency of the patterns to lose their characteristic features, namely their long-lived stability and radial, ringlike structure. Matson *et al.* [8] reported that the patterns ceased to exist for higher values of viscosity than approximately 60 cP.

E. The motion of a single particle

In the theoretical discussion (Sec. III A) we shall make reference to the motion of a single particle in the otherwise rigidly rotating fluid. An additional experiment was therefore carried out to examine a typical trajectory. The experimental system was the same as the one used in the previous experiment to observe the particles' motion from the axial direction. The inner diameter of the tube was 55.8 mm and the frequency of rotation was 0.77 Hz, chosen in the interval where the banding phenomenon was confirmed. The particle used was a polystyrene ball having a diameter of 3 mm. In the analysis of the motion we utilized each of the individual frames, taken at time intervals of 0.02 s, to determine the

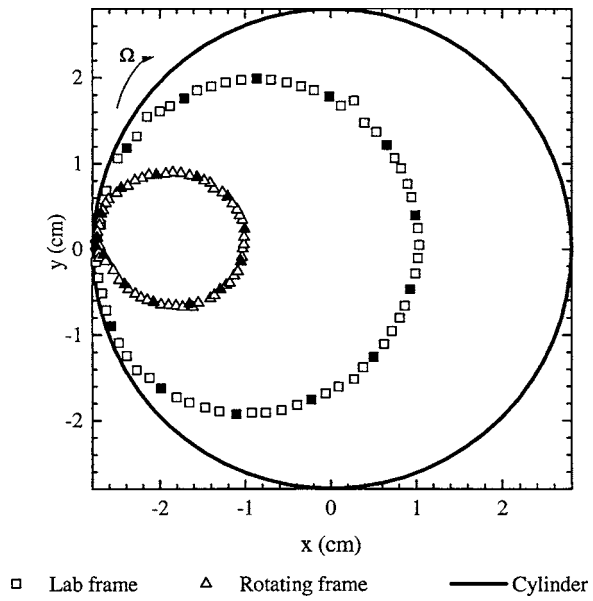

FIG. 9. Projection of the trajectory of a polystyrene particle in a water-filled cylinder. Measurements were made in the laboratory frame (squares) using a CCD camera facing one of the bounding walls of the tube, which was made from transparent material. The results were then converted to the rotating frame (triangles), using the known frequency of the rotating cylinder, Ω. The interval between successive measurements is 0.02 s. The solid symbols mark every fifth data point.

particle's position as a function of time. The results are presented in Fig. 9.

The particle trajectories, both in the laboratory frame and in the rotating frame, are almost circular, adjoining to the tube surface. The sense of rotation as seen in the laboratory frame is clockwise, while the rotating frame sense is anticlockwise. An estimate of the rate of the circular motion can be drawn from the solid symbols which mark every fifth point. These indicate that to a good degree the particle maintains a uniform velocity. The frequency of rotation was found to be approximately that of the bounding tube (to within 1.5% of Ω).

III. THEORETICAL ANALYSIS

A complete analytical solution to the problem of a self-organizing system of particles suspended in a rotating fluid-filled tube is obviously a formidable task. Thus when addressing the problem we have to make some simplifying assumptions. In general, our approach to the problem, based on the assumption of a dilute suspension, consists of decoupling the motion of the dispersed phase from that of the continuous phase [12]. In other words, we start by studying the gravity-induced motion of the suspended particles through looking first at the problem of a single particle in a rotating drum, under the influence of gravity. Then we take the information gained and implement it into the governing Navier-Stokes equation for the fluid.

A. Trajectory of a suspended particle

The forces acting on the suspended particle (in the laboratory frame of reference) during its motion through the rigidly rotating bulk of fluid are the gravity force $\mathbf{F}_G$, the force due to the pressure gradient in the suspending fluid $\mathbf{F}_C$, and the drag force $\mathbf{F}_D$ (Fig. 10). Breu *et al.* [7] studied the trajectory of a suspended spherical particle for low Re (based on the particle size and on its relative velocity with respect to the fluid) and have shown that it resembles that of a falling body in a quiescent viscous fluid. For relatively high Re, the drag on a particle in an unsteady motion is in general not known. Nevertheless the overall effect in our configuration is to cause the trajectory to tend to close on itself due to the increasing dominance of the drag force. This indeed is the case observed for the polystyrene ball moving through the rotating fluid in an almost circular motion, with an effective frequency approximately equal to that of the rotating tube (Fig. 9). The Reynolds number in this specific case was Re ≈ 50. With respect to the rotating frame of reference, regardless of Re, the suspended particles can be seen as the cause of a time-dependent periodic disturbance to the otherwise unperturbed continuous phase.

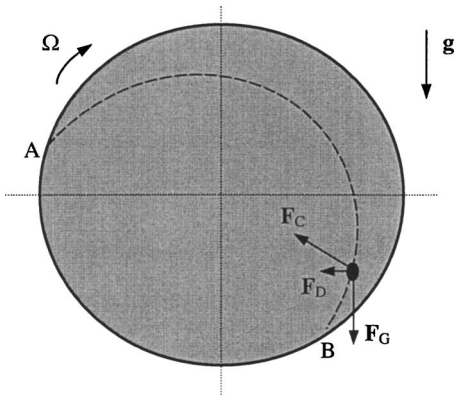

FIG. 10. Forces acting on a suspended particle in a rotating, fluid-filled, horizontal cylinder. The fluid is assumed to be in solid body rotation. The particle detaches from the surface at A and rejoins at B. The particle then acquires its initial velocity going back from B to A.

B. The continuous phase—Inertial waves

Turning to the continuous phase, we consider an incompressible viscous fluid. The Navier-Stokes equations, with reference to a coordinate system rotating with angular velocity $\mathbf{\Omega}$, are

$$\frac{\partial \mathbf{u}}{\partial t} + (\mathbf{u}\cdot\nabla)\mathbf{u} + 2\mathbf{\Omega}\times\mathbf{u} = -\nabla\tilde{p} + \upsilon\nabla^2\mathbf{u},$$
$$\nabla\cdot\mathbf{u} = 0, \tag{1}$$

where υ is the kinematic viscosity and $\tilde{p}$ is the reduced pressure, incorporating the dynamical pressure and the centrifugal and gravity effects:

$$\tilde{p} = \frac{p}{\rho} - \frac{1}{2}(\mathbf{\Omega}\times\mathbf{r})^2 - \mathbf{g}\cdot\mathbf{r}. \tag{2}$$

We use the following scaled variables:

$$\mathbf{r}^* = \frac{\mathbf{r}}{R}; \quad t^* = \Omega t; \quad \mathbf{u}^* = \frac{\mathbf{u}}{U}; \quad \hat{\mathbf{k}} = \frac{\mathbf{\Omega}}{\Omega}; \quad p^* = \frac{\tilde{p}}{\Omega U R}, \tag{3}$$

U being the characteristic perturbation velocity. Equation (1) can then be put in dimensionless form:

$$\frac{\partial \mathbf{u}^*}{\partial t^*} + \varepsilon(\mathbf{u}^* \cdot \boldsymbol{\nabla}^*)\mathbf{u}^* + 2\hat{\mathbf{k}} \times \mathbf{u}^* = -\boldsymbol{\nabla}^* p^* + E\boldsymbol{\nabla}^{*2}\mathbf{u}^*,$$
$$\boldsymbol{\nabla}^* \cdot \mathbf{u}^* = 0, \tag{4}$$

here the Rossby number, $\varepsilon = U/\Omega R$, indicates the relative weight of the nonlinear and Coriolis terms, and the Ekman number, $E = \upsilon/\Omega R^2$, the relative weight of the viscous and Coriolis terms. We now assume[3] an almost inviscid fluid ($E \ll 1$) and that the perturbation caused by the suspended particles is small ($\varepsilon \ll 1$), and arrive at the following linearized set of equations for the reduced-pressure and velocity components in cylindrical coordinates (taking $\hat{\mathbf{k}} = \hat{\mathbf{z}}^*$):

$$\frac{\partial u_r^*}{\partial t^*} - 2u_\phi^* = -\frac{\partial p^*}{\partial r^*},$$
$$\frac{\partial u_\phi^*}{\partial t^*} + 2u_r^* = -\frac{1}{r^*}\frac{\partial p^*}{\partial \phi^*},$$
$$\frac{\partial u_z^*}{\partial t^*} = -\frac{\partial p^*}{\partial z^*}, \tag{5}$$
$$\frac{1}{r^*}\frac{\partial (r^* u_r^*)}{\partial r^*} + \frac{1}{r^*}\frac{\partial u_\phi^*}{\partial \phi^*} + \frac{\partial u_z^*}{\partial z^*} = 0.$$

As the suspended particles are believed to be the source of a time periodic disturbance to the otherwise rigidly rotating fluid we ascribe the velocity and reduced pressure fields the form:

$$(u_r^*, u_\phi^*, u_z^*, p^*) = [U^*(\mathbf{r}^*), V^*(\mathbf{r}^*), W^*(\mathbf{r}^*), P^*(\mathbf{r}^*)]\exp(i\alpha t^*),$$

which, by substitution into Eq. (5) gives:

$$i\alpha U^* - 2V^* = -\frac{\partial P^*}{\partial r^*},$$
$$i\alpha V^* + 2U^* = -\frac{1}{r^*}\frac{\partial P^*}{\partial \phi^*},$$
$$i\alpha W^* = -\frac{\partial P^*}{\partial z^*}, \tag{6}$$
$$\frac{1}{r^*}\frac{\partial (r^* U^*)}{\partial r^*} + \frac{1}{r^*}\frac{\partial V^*}{\partial \phi^*} + \frac{\partial W^*}{\partial z^*} = 0,$$

and from which a second order differential equation for the effective pressure can be derived:

$$\left[\frac{\partial^2}{\partial r^{*2}} + \frac{1}{r^*}\frac{\partial}{\partial r^*} + \frac{1}{r^{*2}}\frac{\partial^2}{\partial \phi^{*2}} + \left(1 - \frac{4}{\alpha^2}\right)\frac{\partial^2}{\partial z^{*2}}\right]P^* = 0. \tag{7}$$

For $\alpha > 2$ the governing differential equation for the pressure is of elliptic type—that is Laplace's equation under scaling of the z coordinate. For $\alpha < 2$, on the other hand, the governing equation is of hyperbolic type and thus the scenario is quite different. The equation is now a wave equation with the z coordinate playing the role of time (Poincaré equation[4]) As mentioned above, the experimental data indicates that segregation is associated with $\alpha \cong 1$ (i.e., the frequency of disturbance is close to the rotation frequency) and thus we assume in the following that the governing equation is hyperbolic.

Next we seek a standing wave solution. We start with Eq. (7) and further assume the following spatial dependence: $f(r^*)\exp[i(m\phi^* + kz^*)]$. Inserting this into Eq. (7) gives Bessel's equation of order m:

$$r^{*2}\frac{d^2 f}{dr^{*2}} + r^*\frac{df}{dr^*} + (\gamma^2 r^{*2} - m^2)f = 0, \tag{8a}$$

where

$$\gamma^2 \equiv k^2\left(\frac{4}{\alpha^2} - 1\right). \tag{8b}$$

As m has to be an integer (requirement of periodicity with respect to ϕ^*), the only relevant solution of the above is the Bessel function of the first kind of order m (the second solution being the Bessel function of the second kind of order m, which diverges for $r^* = 0$). We thus have for the pressure,

$$P^* = P_0 J_m(\gamma r^*)\exp[i(m\phi^* + kz^*)], \tag{9}$$

where P_0 is an amplitude. The corresponding velocity components are

$$U^* = -i\frac{\gamma P_0}{4 - \alpha^2}\left[2m\frac{J_m(\gamma r^*)}{\gamma r^*} + \alpha J_m'(\gamma r^*)\right]\exp[i(m\phi^* + kz^*)],$$
$$V^* = \frac{\gamma P_0}{4 - \alpha^2}\left[2J_m'(\gamma r^*) + m\alpha\frac{J_m(\gamma r^*)}{\gamma r^*}\right]\exp[i(m\phi^* + kz^*)], \tag{10}$$
$$W^* = -\frac{kP_0}{\alpha}J_m(\gamma r^*)\exp[i(m\phi^* + kz^*)].$$

The boundary conditions now have to be implemented. The condition at the vertical walls, $W^*(z^* = 0, L/R) = 0$, is satisfied by a superposition of two similar waves, having wave numbers equal in magnitude and given by

[3] Discussion of the validity of these assumptions with regard to the experiments will be given in Sec. V.

[4] Named after H. Poincaré for his pioneering work [13].

$$k_n = \frac{n\pi R}{L}, \quad n = \pm 1, \ \pm 2, \ \pm 3, \ldots, \tag{11}$$

which propagate in opposite axial directions.

At the curved cylindrical surface we have $U^*=0$ on $r^*=1$, yielding (using the analytical relationship between J'_m, J_m, and J_{m-1}):

$$\gamma J_{m-1}(\gamma) + m\left(\frac{2}{\alpha} - 1\right) J_m(\gamma) = 0 \tag{12}$$

or, using Eq. (8b):

$$\gamma J_{m-1}(\gamma) + m(\sqrt{1 + (\gamma L/n\pi R)^2} - 1) J_m(\gamma) = 0. \tag{13}$$

Equation (13) together with Eqs. (8b) and (11) determine, for a given tube (that is, given R and L), the eigenfrequencies α_{lmn} [l being the index corresponding to the roots of Eq. (13)].

IV. CONFIRMATION OF THEORETICAL APPROACH

We are now in a position to interpret the experimental observations in light of the foregoing theoretical approach. We argue that the segregation of the particles is a manifestation of an inertial mode. First, we recall that in the natural circumstances, all excited inertial modes are bound to decay in the spin-up time, $t_{SU} \approx L/(\upsilon\Omega)^{1/2}$ [14], which is typically 1 to 2 min in our configuration. However, gravity, by means of its induced effect on the particles' motion, is able to continuously excite modes with angular frequency $\alpha \cong 1$. Of particular relevance are the resonant modes with $m=1$ because the combination ϕ^*+t^* yields a stationary flow field in the laboratory frame of reference.

Denoting the inertial mode wavelength in the axial (z) direction by λ, we have, utilizing Eqs. (8b) and (12):

$$\gamma J_0(\gamma) + \left(\frac{2}{\alpha} - 1\right) J_1(\gamma) = 0, \tag{14a}$$

$$\frac{\lambda}{R} = \frac{2\pi}{\gamma}\sqrt{\frac{4}{\alpha^2} - 1}. \tag{14b}$$

Considering the first root of Eq. (14a), we find that λ/R varies from 3.26 to 4.20 when α changes between 1.18 and 0.95, which is in good agreement with the scaled experimental periodic length (Λ/R) observed in Figs. 4 and 8. Consecutive roots yield decreasing values for λ/R. The observed fact that there is an interval of periodic lengths (Figs. 4 and 8) rather than a single value, as would be expected for a discrete frequency excitation, might be attributed to the large number of particles participating in the mode excitation. This would mean that a band of frequencies is excited in the vicinity of $\alpha=1$, each frequency in the band corresponding to a different resonant tube length.

In the particular case for which the tube radius is given ($r^*=1$) and $\alpha=m=1$, the dimensionless velocity components of the inertial modes are

$$u_r^* = V_0\left[2\frac{J_1(\gamma r^*)}{\gamma r^*} + J_1'(\gamma r^*)\right]\sin(\phi^* + t^*)\cos(kz^*),$$

$$u_\phi^* = V_0\left[2J_1'(\gamma r^*) + \frac{J_1(\gamma r^*)}{\gamma r^*}\right]\cos(\phi^* + t^*)\cos(kz^*), \tag{15}$$

$$u_z^* = \sqrt{3}V_0 J_1(\gamma r^*)\sin(\phi^* + t^*)\sin(kz^*),$$

where $V_0 \equiv 2k^2 P_0/\gamma$, and γ and k are determined by Eqs. (14a) and (8b), respectively. The first root of Eq. (14a) is $\gamma = 2.74$ yielding a wavelength $\lambda/R = 3.97$. The tube lengths corresponding to inertial mode vibrations are given by $L/R = 1.985|n|$.

In Fig. 11 we present the velocity field (15) for the inertial mode (1,1,3) in the vertical plane through the axis of rotation, at $t^*=0$. The arrows in the figure represent both the relative magnitude and the direction of the velocity field. The figure suggests that the suspended particles, initially exciting the inertial mode, are carried by the axial component of the fluid to the loci of $W^*=0$.

The fact that the observed periodic spacing corresponds to the wavelength as opposed to half-wavelength (as it does, for instance, for Kundt's tube) might be related to the correlation between the flow field in alternate $r-\phi$ nodal planes and the gravity-induced motion of the suspended particles. Figure 12 shows the calculated velocity field in the $r-\phi$ nodal planes at $z=\pi/k$ and $z=0$ at $t^*=0$, both in the rotating and in the laboratory frames of reference. In the former plane there is a good correlation between the theoretical field and the observed off-centered ring of Figs. 7(a) and 9, imposing an appropriate velocity pattern on its circumference. The flow field in the latter plane does not correlate the particles' trajectory. If the same number of particles were in either kind of nodes, the resultant flow would cancel and there would be no segregation. The fact that at the walls one can have either of the two flow patterns shown in the right column of Fig. 12, together with the fact that the gravity induced trajectory of the particles correlates only one of those, lead to two degenerate states for each resonant tube length.

Visualizing the actual flow field would obviously be valuable to confirm the validity of the theoretical approach. To this end we performed an experiment with 1 mm glass beads suspended in a 7 cP water-glycerol solution. As a result of

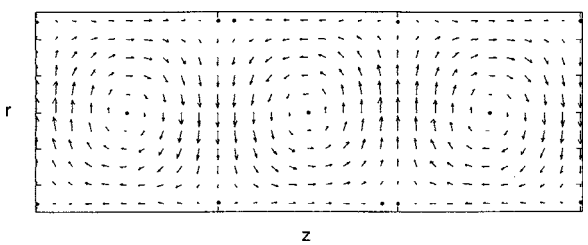

FIG. 11. Visualization of the velocity field in the vertical plane through the axis for the inertial mode (1,1,3), at $t^*=0$. The arrows drawn represent the direction and relative magnitude of the velocity field.

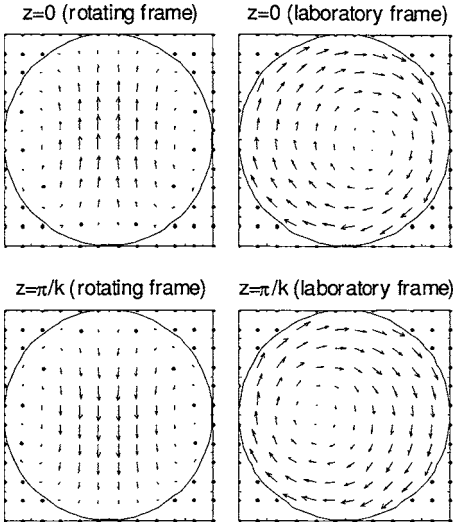

FIG. 12. Visualization of the velocity field in the nodal planes $z=0$ and $z=\pi/k$ in rotating and in laboratory frames of reference. In these planes the axial component $W^*=0$. The perturbation amplitude used in the calculation of the velocity field in the laboratory frame is $V_0=0.2$ (scaled by the unperturbed velocity at the circumference).

stirring of the two components the fluid contained tiny air bubbles, which played the role of tracers of the flow field and thus allowed its photographic capture.

The experimental setup used was the same as that used in the investigation of the dependence of the periodic length on tube length (Fig. 2), except that now the only illumination was a thin light sheet directed from above in the vertical plane through the axis of rotation. In Fig. 13 we present the photograph of the illuminated volume together with a visualization of the predicted flow due to the existence of the inertial wave. The predicted flow field is seen to be in good agreement with the observed one. A video clip taken of the same illuminated volume [11] confirms the predicted sense of circulation between neighboring nodes.

Inertial waves were observed in the past in the configuration of a rotating cylinder using injected dye, revealing general features of the flow pattern [15,16]. This is a visualization of the actual flow field pertaining to an inertial mode, from which a detailed velocity field can in principal be obtained.

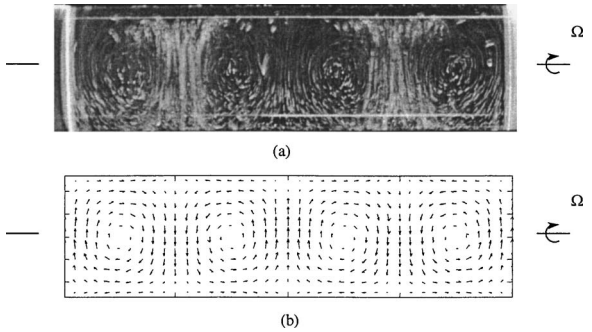

FIG. 13. Projection of the velocity field on the vertical plane through the axis of rotation for the (1,1,4) mode (laboratory frame of reference). (a) Photographic capture of the flow field using a 3 mm light sheet. The relatively large white blobs seen are the glass balls causing the excitation of the inertial wave. The thin streaks represent the trajectory of the small air bubbles (tracers). (b) Visualization of the theoretical field corresponding to the same mode.

V. DISCUSSION

The banding phenomenon of suspended particles in a rotating horizontal cylinder has been investigated both experimentally and theoretically. The experimental investigation focused on a dilute, low viscosity suspension containing millimeter-sized solid particles. The experiments indicate a robust phenomenon independent of particle characteristic and tube diameter (Fig. 4). The effects of viscosity were shown to be minor up to a value of 10 cP (Fig. 8). A theoretical framework was given which suggests a mechanism leading to banding. In the theory the suspended particles are the source of a periodic time dependent perturbation (in the rotating frame of reference) to the otherwise quiescent fluid. This disturbance excites inertial modes in the rotating bounded fluid. Of particular importance is the inertial mode corresponding to excitation at a frequency close to Ω, and which when viewed from the laboratory frame seems stationary. The circulation in the vertical plane through the axis of rotation corresponding to this mode (Fig. 11) is believed to be the cause of segregation into alternate nodes of the mode. The periodic length is thus predicted to be equal to the wavelength of the inertial mode, $\lambda \cong 4R$; in good agreement with the observed periodic length (Figs. 4 and 8). The theoretical predictions were further confirmed by a photographic capture of the projection of the velocity field on the vertical plane through the axis (Fig. 13).

The two simplifying assumptions of an inviscid, linearly perturbed fluid, which enabled the physical insight into the origin of the banding mechanism, represent the first step in a complex singular perturbation procedure.[5] The assumed smallness of the Ekman number ($E \ll 1$) can be shown to be consistent with the relevant experimental parameters. If we assume that we indeed have a standing wave then the characteristic length will be the order of the wavelength, which in our case is the order of the tube's radius. We therefore can write

$$E = \frac{v}{\Omega \mathcal{L}^2} = \frac{v}{\Omega \lambda^2} \approx \frac{v}{\Omega R^2}. \tag{16}$$

For the case of suspended particles in water ($v \cong 0.01$ cm^2/s), the angular frequency of rotation is about 10 rad/s, thus taking $R \approx 1$ cm:

$$E = 10^{-3}.$$

Hence we see that the viscous term is indeed negligible in the interior. The viscous effects are confined to small domains near the walls (in particular the important Ekman boundary layers). Moreover, we learn from Eq. (16) that for values of viscosity appreciably higher than ten times that of

[5] A detailed account of the particular case for which $\varepsilon \ll E^{1/2} \ll 1$ is given by Greenspan [14].

water the theoretical framework presented will not be a valid one. This last prediction is in agreement with the observed tendency of the bands to be unstable for values higher than 10 cP, mentioned in Sec. II D.

While the above estimate agrees with previous works of Lipson and Seiden [6] and of Breu *et al.* [7], the corresponding Ekman number for the experiments carried out by Matson *et al.* [8] is $E \approx 0.1$. This intermediate value implies that the viscous term is not negligible. However, inertial effects such as those considered here have to be taken into account in addressing their experiments. Indeed, the flow pattern which is visible in the experiments of Matson *et al.* is consistent with the present interpretation. In addition these authors report that "The trajectory center follows a zigzag path, being closer to the upgoing wall for the $r-\theta$ planes with the highest particle densities and closest to the downgoing wall for the smallest particle densities," which exactly describes the zero-velocity axis (in the horizontal plane) in our model.

The Rossby number ε, indicating the relative importance of the nonlinear term in Eq. (4), or equivalently, the ratio of the dimensional perturbation amplitude to the container velocity (ΩR), can in principle be adjusted by varying the rotation frequency of the bounding cylinder though ideal conditions for segregation into bands seem to correspond to nonnegligible values. Formally, Eq. (5) is derived through taking the first component of the perturbation series in powers of ε:

$$\mathbf{u}^*(\mathbf{r}^*,t^*,E,\varepsilon) = \sum_{n=0}^{\infty} \mathbf{u}^{*(n)}(\mathbf{r}^*,t^*,E)\varepsilon^n,$$
$$p^* = \sum_{n=0}^{\infty} p^{*(n)}(\mathbf{r}^*,t^*,E)\varepsilon^n. \tag{17}$$

It will be instructive to study the yet unexplored influence of higher orders in Eq. (17) on the flow. In particular, such a study might shed light on the physical origin of the phenomenon of oscillations between two possible band patterns.

The fact that in some instances periodic lengths approximately equal to half the value of $4R$ were observed for small particles ($\approx 100\ \mu$m) might be attributed to their relatively strong tendency to adhere to the flow field and act as tracers. This would mean that changes in particle concentration along the axis of rotation would be more moderate, and, in particular, that in the interleaving nodal planes (e.g., the $z=0$ plane in Fig. 12) there would be a noticeable concentration, as a result of the converging character of the flow field (Fig. 11).

Our discussion has focused on positively buoyant particles though banding of negatively buoyant particles was observed (i.e., air bubbles suspended in water [6]). The situation in this case is symmetrical to the one with positively buoyant particles as now the force due to gravity changes its sign. Thus, with reference to Fig. 9, the particle will detach from the bounding surface at a point in the fourth quarter and, going through a symmetrical trajectory to the one depicted, will reunite at a point on the upper part of the tube. This fact is neatly confirmed by the observed tendency of positively and negatively buoyant particles, suspended in the same fluid-filled tube, to segregate into alternate nodal planes [10].

We believe the results of the present work might find further applications not only in industrial applications such as centrifuge separation, but also in related fields such as astrophysics and geophysics where mechanisms of aggregation for solid particles, suspended in a rotating bulk of fluid, are sought (e.g., dust aggregation in protoplanetary accretion disks).

ACKNOWLEDGMENTS

We wish to thank Professor J. Franklin for his valuable help with the theoretical analysis and S. Hoida for his technical assistance. This work was supported by the Minerva Foundation for Non-Linear Science and by the Technion Vice-President's Fund for the Promotion of Research. G.S. acknowledges the support of a Neeman Scholarship.

[1] O. Zik *et al.*, Phys. Rev. Lett. **73**, 644 (1994).
[2] N. Jain, D. V. Khakhar, R. M. Lueptow, and J. M. Ottino, Phys. Rev. Lett. **86**, 3771 (2001).
[3] M. Tirumkudulu, A. Tripathi, and A. Acrivos, Phys. Fluids **11**, 507 (1999).
[4] M. Tirumkudulu, A. Mileo, and A. Acrivos, Phys. Fluids **12**, 1615 (2000).
[5] S. G. Lipson, J. Phys.: Condens. Matter **13**, 5001 (2001).
[6] S. G. Lipson and G. Seiden, Physica A **314**, 272 (2002).
[7] A. P. J. Breu, C. A. Kruelle, and I. Rehberg, Europhys. Lett. **62**, 491 (2003).
[8] W. R. Matson, B. J. Ackerson, and P. Tong, Phys. Rev. E **67**, 050301 (2003).
[9] J. Lee and A. J. C. Ladd, Phys. Rev. Lett. **89**, 104301 (2002).
[10] G. Seiden, S. G. Lipson, and J. Franklin, Phys. Rev. E **69**, 015301 (2004).
[11] See EPAPS Document No. E-PLEEE8-72-164508. A direct link to this document may be found in the online article's HTML reference section. The document may also be reached via the EPAPS homepage (http://www.aip.org/pubservs/epaps.html) or from ftp.aip.org in the directory /epaps/. See the EPAPS homepage for more information.
[12] M. Ungarish, *Hydrodynamics of Suspensions* (Springer, New York, 1993).
[13] H. Poincaré, Bull. Astron. **27**, 321 (1910).
[14] H. P. Greenspan, *The Theory of Rotating Fluids* (Breukelen Press, Brookline, 1990).
[15] D. Fultz, J. Meteorol. **16**, 199 (1959).
[16] T. Ito, Y. Suematsu, T. Hayase, and T. Nakahama, Bull. JSME **27**, 458 (1984).